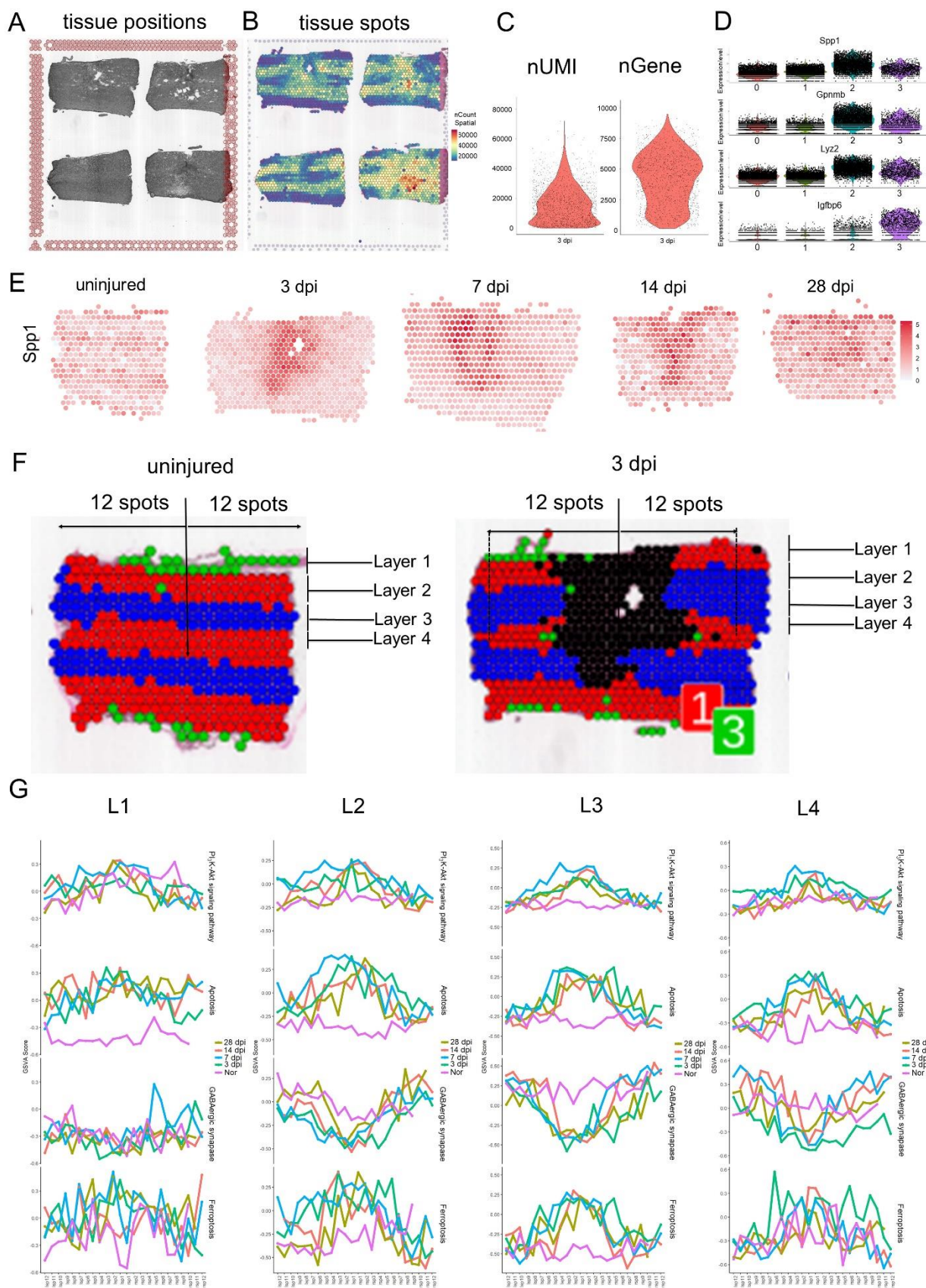
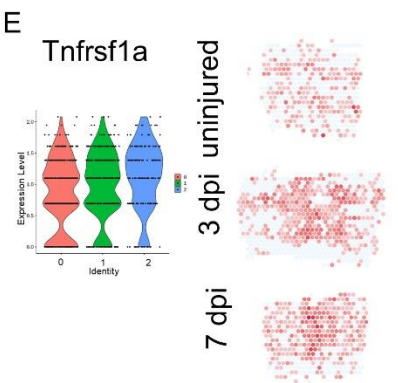
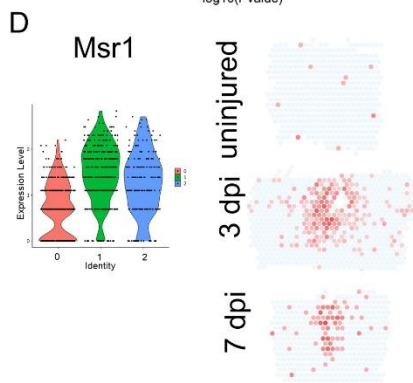
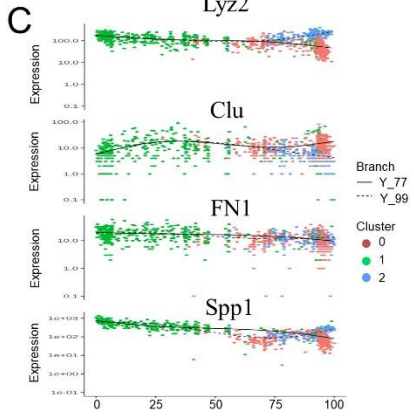
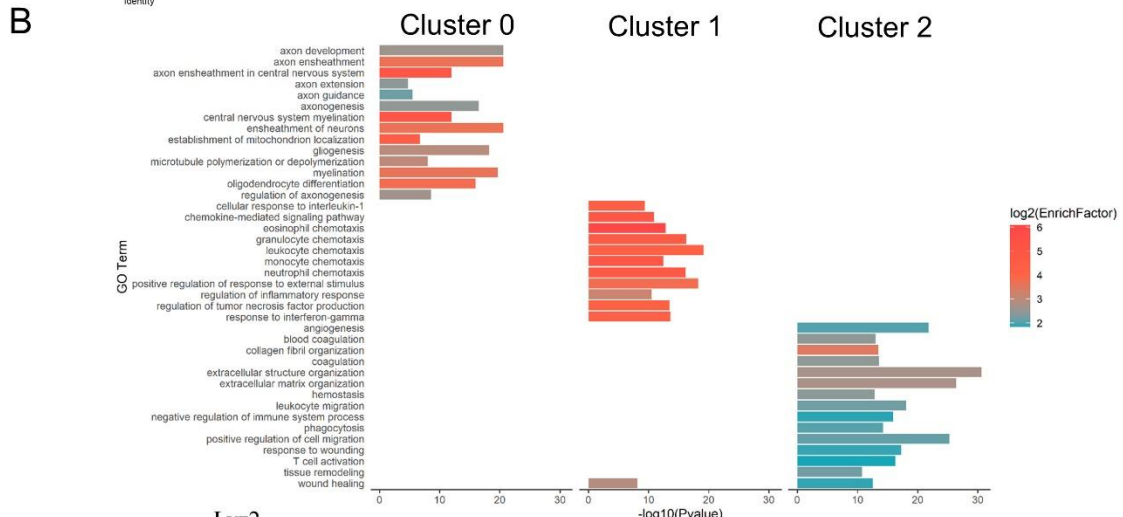
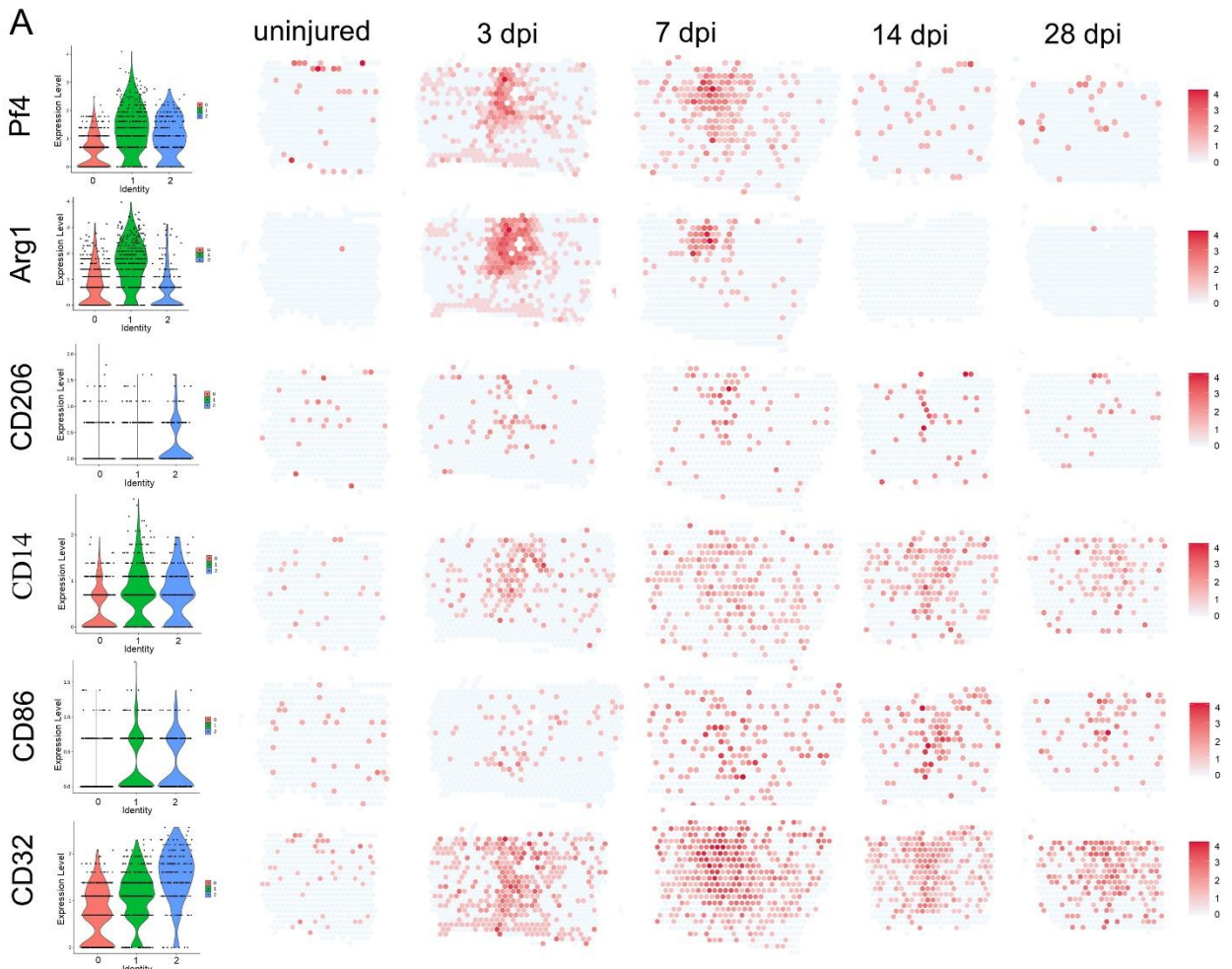


# Supplementary Materials



**Fig. S1 Quality control and spatial distribution of spots involved in glial scar formation. A** Representative images of section positions from samples at 3 dpi. **B** Representative images of the captured spots in sections from samples at 3 dpi. **C** Violin plots showing nUMI and nGene in sections from the samples at 3 dpi. **D** Violin plots showing representative genes of cluster 2 cells and cluster 3 cells, the scar-associated clusters. **E** Spatial feature plots of *Spp1*, a stress response-associated gene. **F** Symmetrical distribution pattern of cluster 0 cells and cluster 1 cells in normal spinal cord; these cells were divided into four layers from layer 1 to layer 4. Subsequently, these cells in the scar were divided into four layers by similar approaches. **G** Selected Gene Set Variation Analysis terms that were enriched in different layers at different stages of scar maturation. Fisher's exact test was used in the pathway enrichment.



**Fig. S2 Distinct macrophage responses after lateral hemisection of the spinal cord.** **A** Violin plots and spatial maps showing the expression of marker genes at different time points after injury. **B** Selected GO terms that were enriched for each cluster (Fisher's exact test). **C** Scatterplots of expression dynamics of selected genes along pseudotime. **D, E** Violin plots and spatial maps showing the expression of selected genes at different time points after injury.

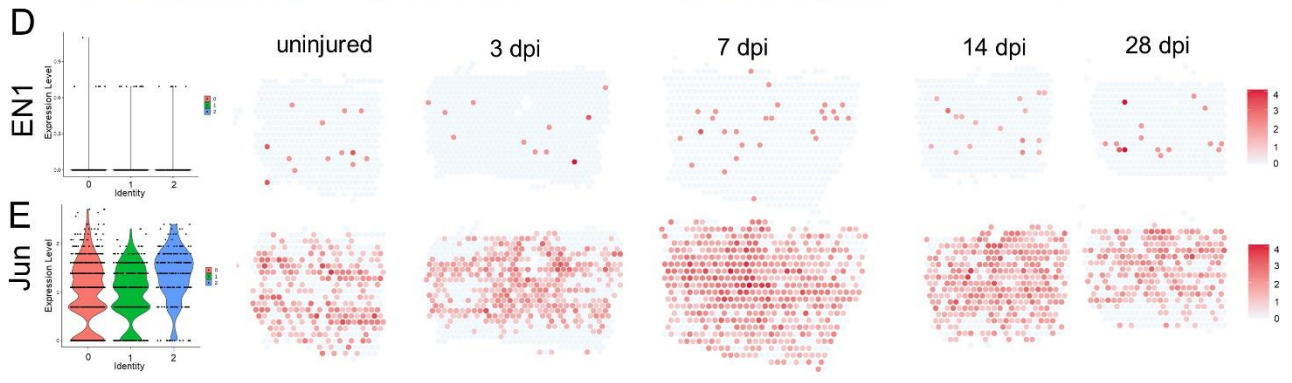
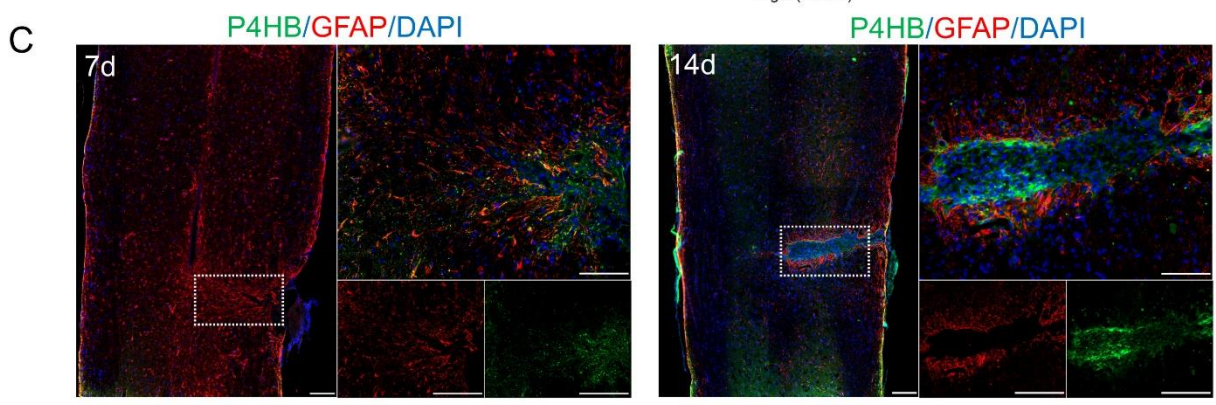
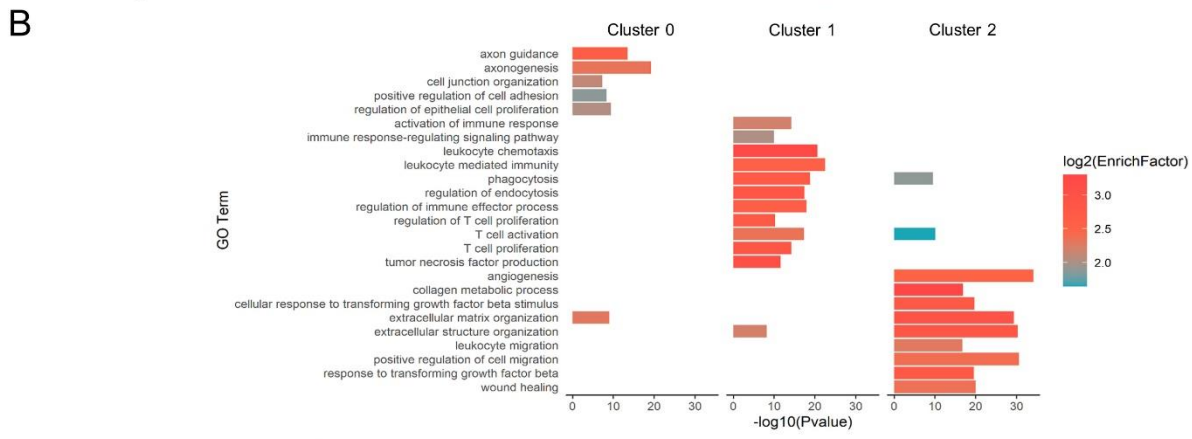
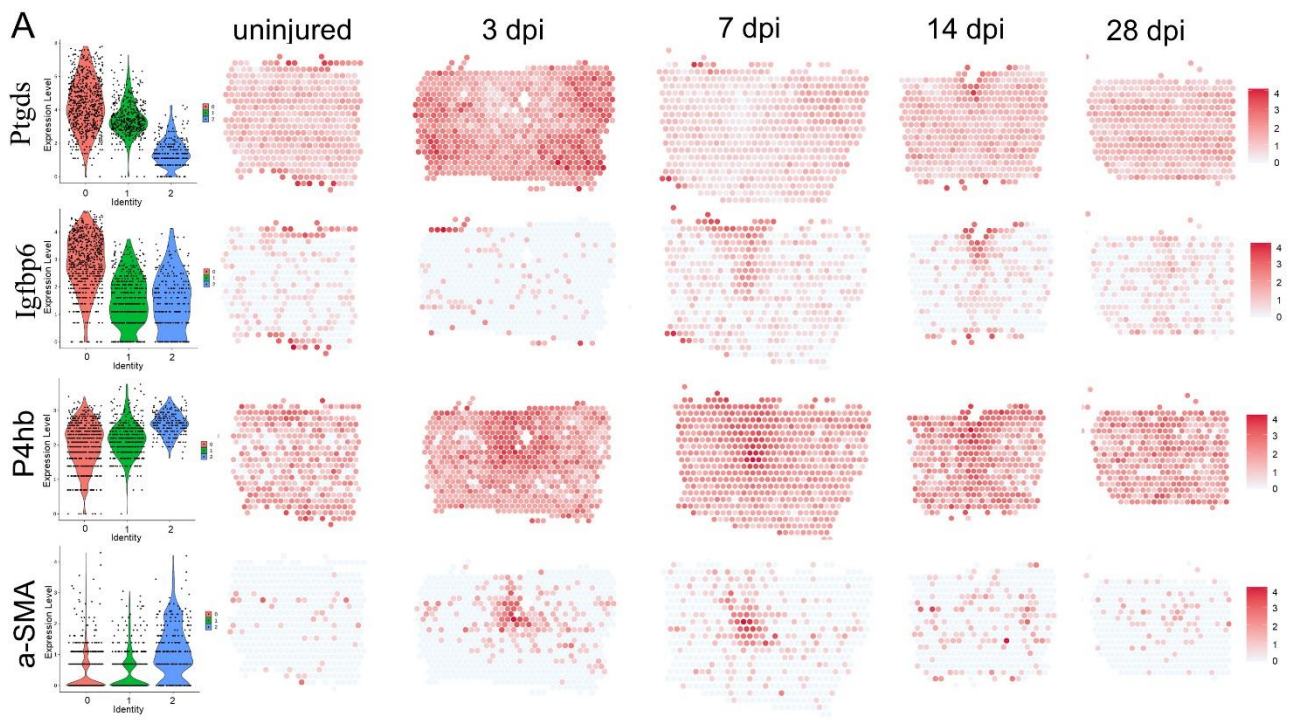


**Fig. S3 Distinct fibroblast responses after lateral hemisection of the spinal cord.** **A** Violin plots and spatial maps showing the expression of selected differentially-expressed genes and marker genes at different time points after injury. **B** Selected GO terms enriched for each cluster (Fisher's exact test). **C** IF-stained 7- and 14-dpi scars for GFAP (red), P4HB (green), and DAPI (blue) confirming the maturation of the scar ( $n = 3$ ; scale bars, 200  $\mu\text{m}$ ). **D** Violin plots and spatial maps showing the expression of *En1* and *Jun*, critical regulators of pathological skin scarring, at different time points after injury.

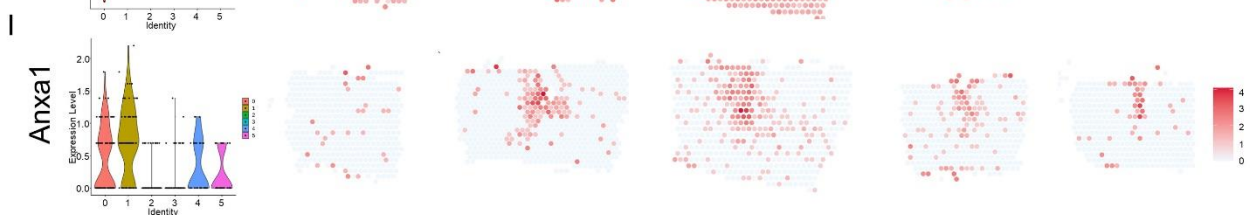
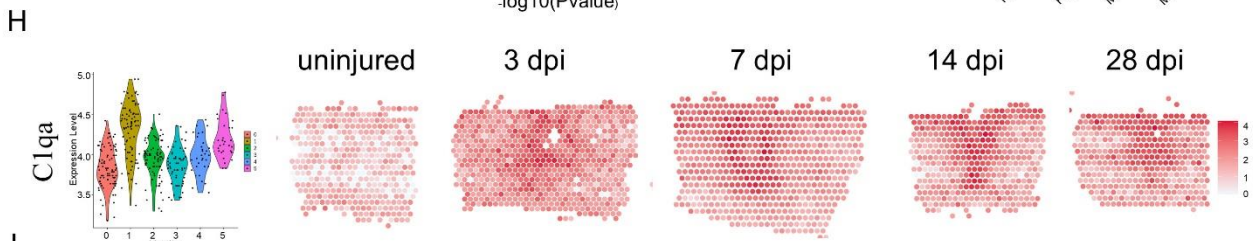
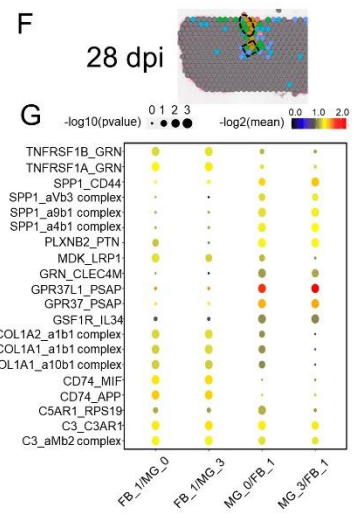
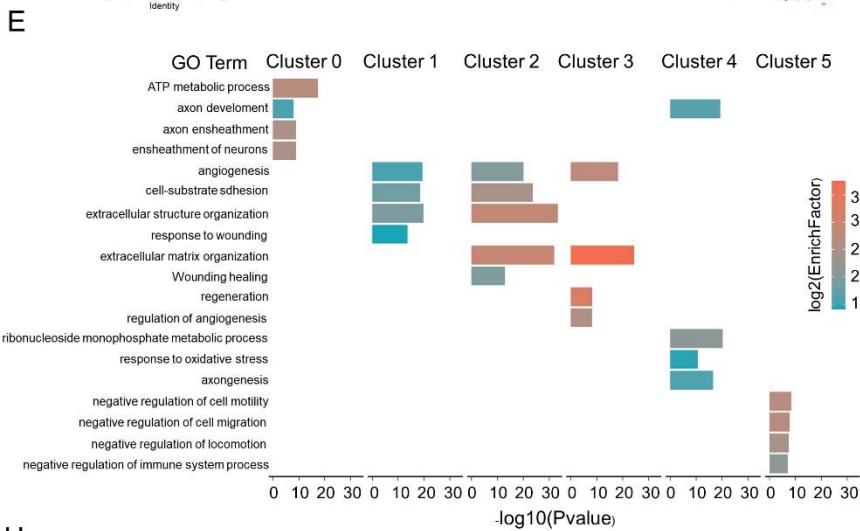
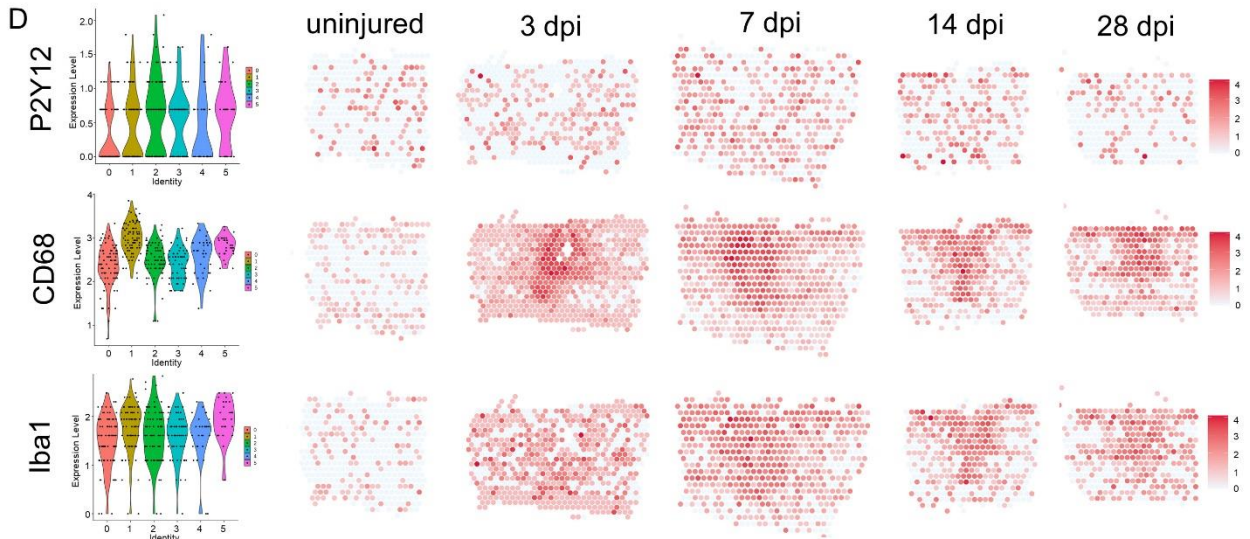
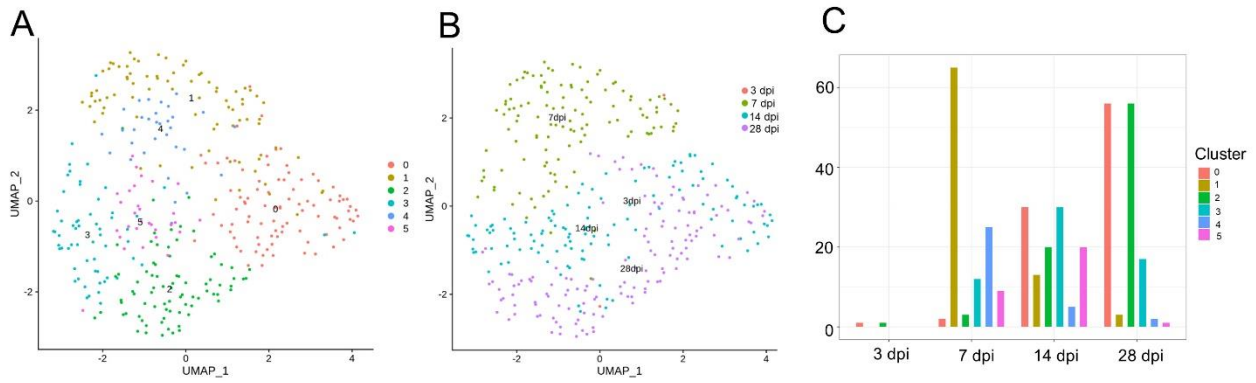


**Fig. S4 Distinct microglial responses after lateral hemisection of the spinal cord.** **A** UMAP spots showing the 3 clusters of microglia in the glial scar. **B** UMAP spots embedding overlay showing the distribution of spots at different time points after injury. **C** Histogram showing the number of spots in each subpopulation at different time points after injury. **D** Violin plots and spatial maps showing the expression of selected marker genes at different time points after injury. **E** Selected GO terms that were enriched for each cluster (Fisher's exact test). **F** Definition of the boundary areas to study the interaction between two neighboring microglia clusters in the scar at 28 dpi. **G** Dot plot of the mean interaction scores between neighboring clusters at 28 dpi. The size of a circle denotes the p-value, and the color denotes the mean interaction score. **H** Violin plots and spatial maps showing the expression of C1q and Anxa1 at different time points after injury.



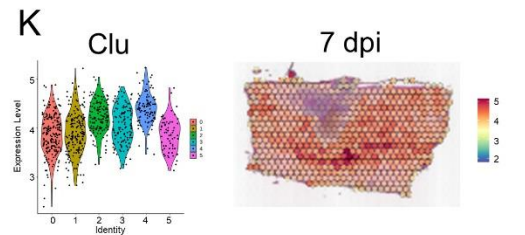
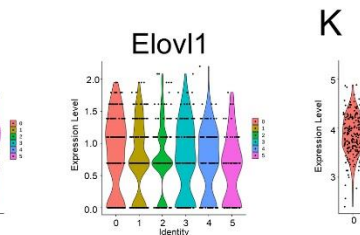
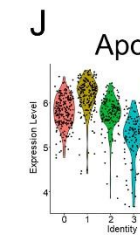
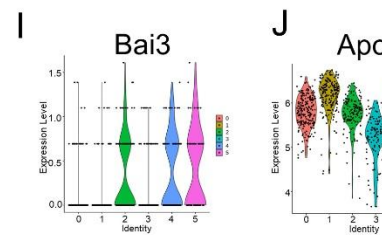
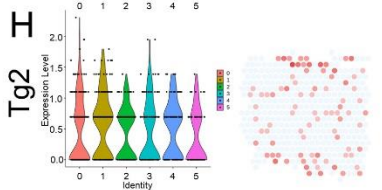
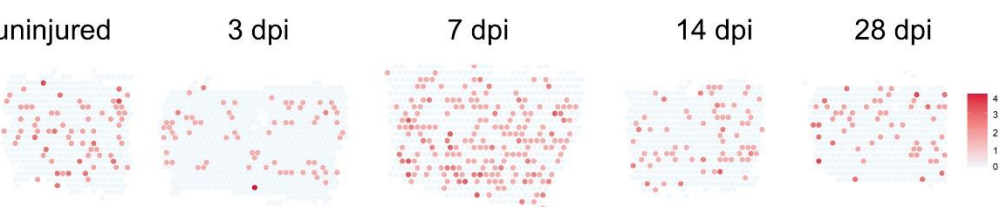
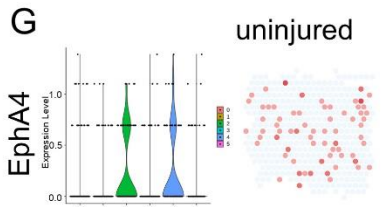
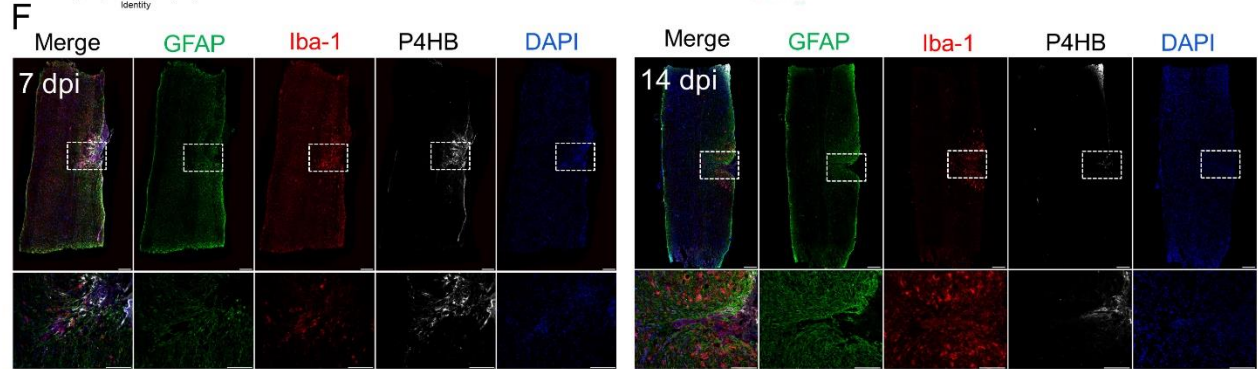
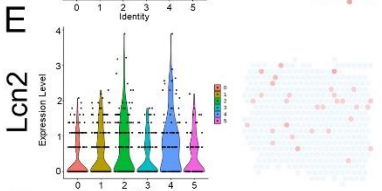
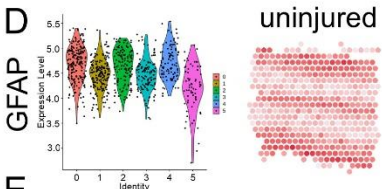
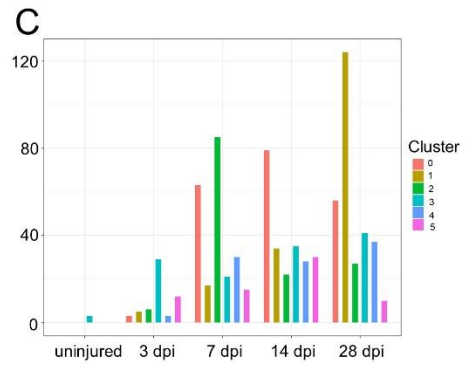
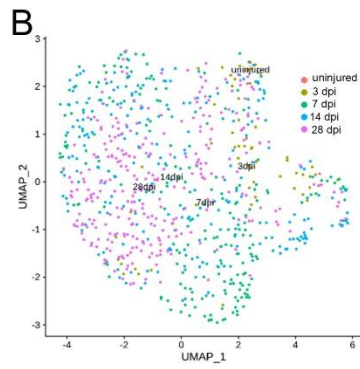
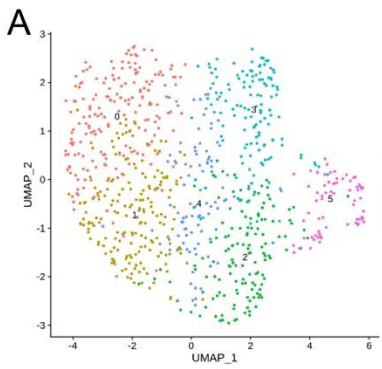


**Fig. S5 Distinct astrocyte responses after lateral hemisection of the spinal cord**

**A** UMAP spots showing the 6 clusters of astrocytes in the glial scar. **B** UMAP spots embedding overlay showing the distribution of spots at different time points after injury. **C** Histogram showing the number of spots in each subpopulation at different time points after injury. **D, E** Violin plots and spatial maps showing the expression of GFAP (**D**) and Lcn2 (**E**) at different time points after injury. **F** IF-stained 7- and 14-dpi scars for GFAP (green), Iba1 (red), P4HB (gray), and DAPI (blue) ( $n = 3$ , scale bar, 200  $\mu\text{m}$ ). **G, H** Violin plots and spatial maps showing the expression of EphA4 (**G**) and Tg2 (**H**) at different time points after injury. **I–K** Violin plots showing the expression of Bai3 (**I**), Apoe and Elov11 (**J**) and Clu in the astrocyte scar after injury.

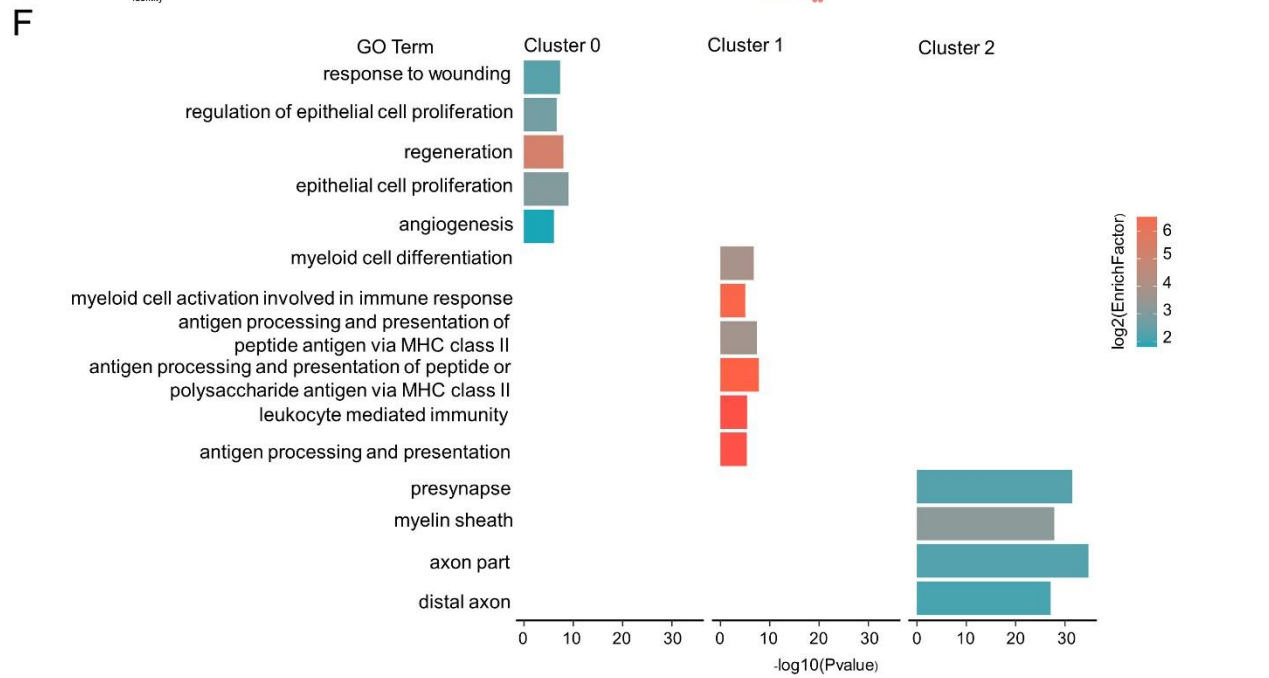
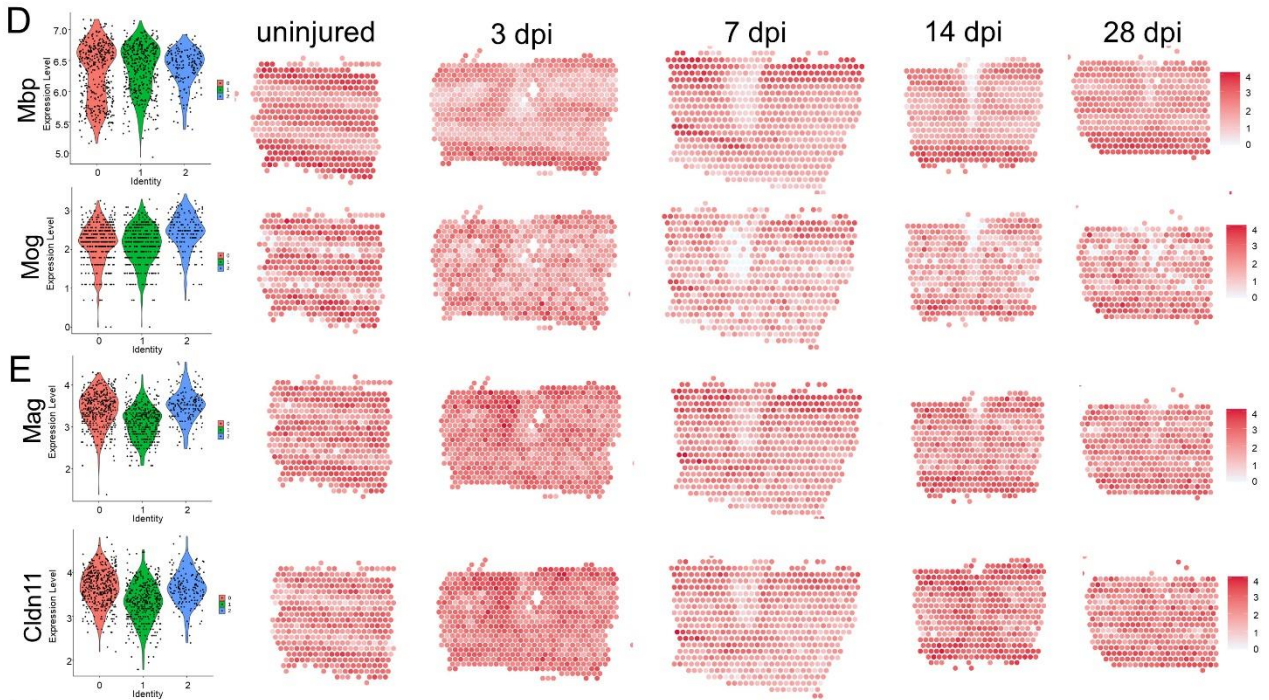
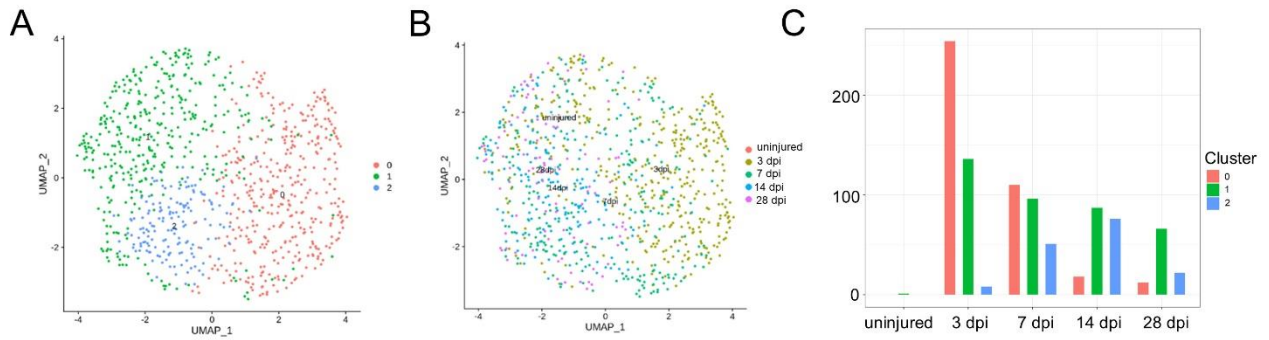
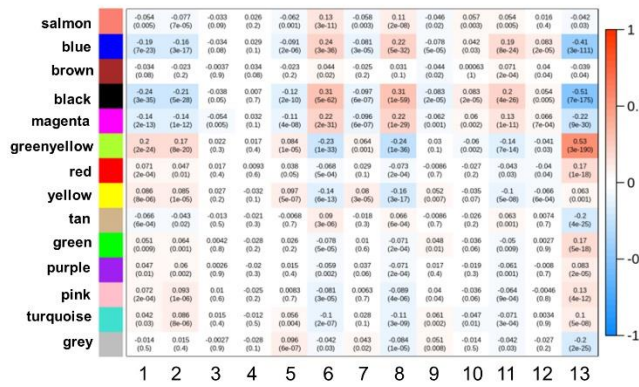


**Fig. S6 Distinct oligodendrocyte responses after lateral hemisection of the spinal cord**

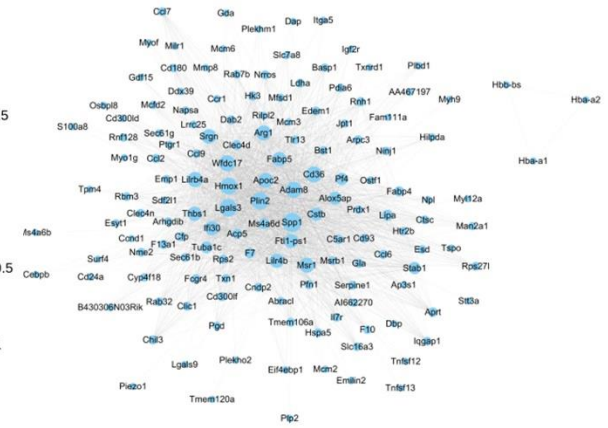
**A** UMAP spots showing the 3 clusters of microglia in the glial scar. **B** UMAP spots embedding overlay showing the distribution of spots at different time points after injury. **C** Histogram showing the number of spots in each subpopulation at different time points after injury. **D, E** Violin plots and spatial maps showing the expression of Mbp and Mog (**D**) and Mag and Cldn11 (**E**) at different time points after injury. **F** Selected GO terms that were enriched for each cluster (Fisher's exact test).

A

Module-trait relationships

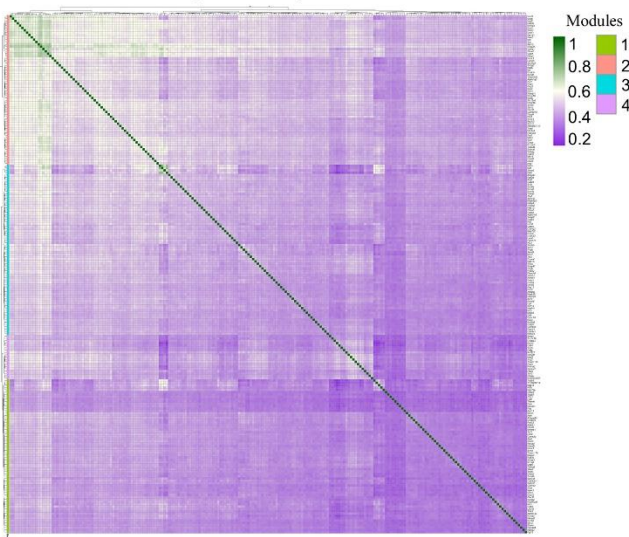


B

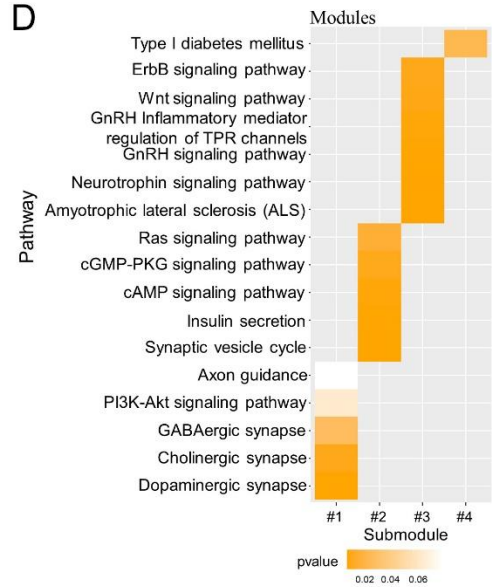


C

Gene-to-gene similarity matrix submodule 3

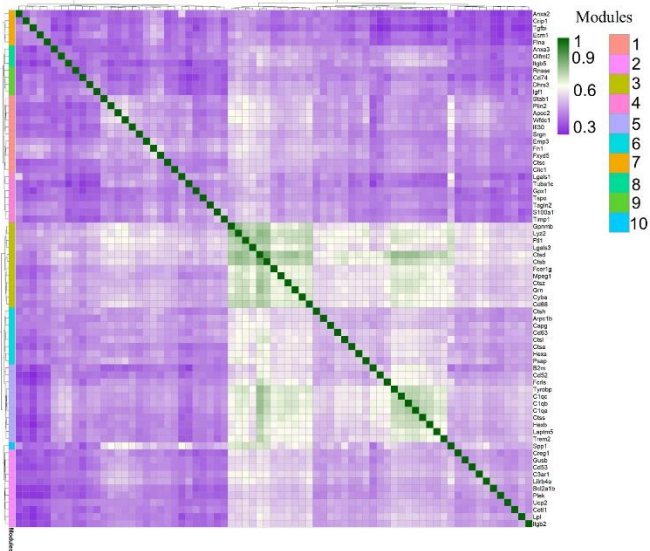


D



E

Gene-to-gene similarity matrix submodule 10



F

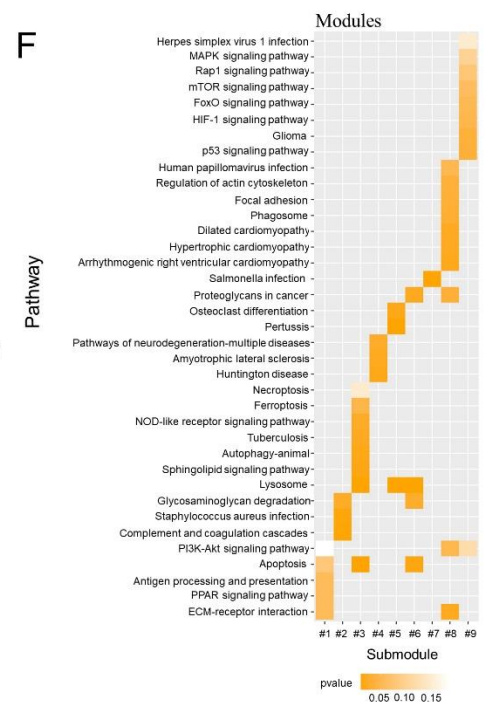


**Fig. S7 Spatiotemporal dynamics of gene expression during maturation of the scar**

**A** Heatmap depicting the correlation scores (digit in the box above) as well as its corresponding P-value (digit in the box below) of modules (rows) and different cell types after injury (columns). 1, astrocytes; 2, microglia; 3, neurons and astrocytes; 4, vascular smooth muscle cells and endothelial cells; 5, fibroblasts; 6, macrophages; 7, astrocytes; 8, oligodendrocytes; 9, astrocytes and oligodendrocytes; 10, endothelial cells; 11, macrophages; 12, fibroblasts; 13, time. **B** Co-expression of selected hub genes enriched in Meblack. The networks were created by Cytoscape. **C** Hierarchical clustering of genes in module 3. **D** Analysis of enriched KEGG pathways among the genes for submodules in **C**. **E** Hierarchical clustering of genes in module 10. **F** Analysis of enriched KEGG pathways among the genes for submodules in **E**.